Direct-CP: Directed Collaborative Perception for Connected and Autonomous Vehicles via Proactive Attention

Yihang Tao[1], Senkang Hu[1], Zhengru Fang[1], and Yuguang Fang[1*]

Abstract— Collaborative perception (CP) leverages visual data from connected and autonomous vehicles (CAV) to enhance an ego vehicle's field of view (FoV). Despite recent progress, current CP methods expand the ego vehicle's 360-degree perceptual range almost equally, which faces two key challenges. Firstly, in areas with uneven traffic distribution, focusing on directions with little traffic offers limited benefits. Secondly, under limited communication budgets, allocating excessive bandwidth to less critical directions lowers the perception accuracy in more vital areas. To address these issues, we propose Direct-CP, a proactive and direction-aware CP system aiming at improving CP in specific directions. Our key idea is to enable an ego vehicle to proactively signal its interested directions and readjust its attention to enhance local directional CP performance. To achieve this, we first propose an RSU-aided direction masking mechanism that assists an ego vehicle in identifying vital directions. Additionally, we design a direction-aware selective attention module to wisely aggregate pertinent features based on ego vehicle's directional priorities, communication budget, and the positional data of CAVs. Moreover, we introduce a direction-weighted detection loss (DWLoss) to capture the divergence between directional CP outcomes and the ground truth, facilitating effective model training. Extensive experiments on the V2X-Sim 2.0 dataset demonstrate that our approach achieves 19.8% higher local perception accuracy in interested directions and 2.5% higher overall perception accuracy than the state-of-the-art methods in collaborative 3D object detection tasks.

I. INTRODUCTION

Collaborative perception (CP) [1]–[3] has emerged as a promising approach to expand the perceptual range of individual vehicles by integrating visual data from multiple connected and autonomous vehicles (CAVs). To effectively monitor road traffic, each CAV is equipped with an array of LiDARs or cameras that capture environmental data from various angles. This information is subsequently synthesized into a bird's eye view (BEV) map, offering a comprehensive representation of a vehicle's surroundings [4]. Nonetheless, relying solely on a single BEV-aided perception system is often insufficient for overcoming blind spots resulted by road obstacles or other CAVs. To address this shortcoming, CP has been adapted to allow multiple CAVs to share their local BEV features, thereby enhancing the accuracy and comprehensiveness of BEV predictions.
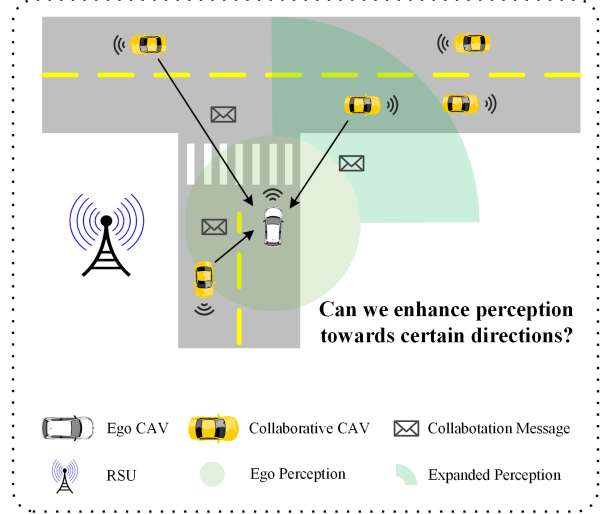
Fig. 1. **Overview of directed CP framework.** Under limited communication budget, ego CAV enhances perception in complex traffic directions while maintaining basic awareness in low-traffic areas.

Currently, most existing studies [5], [6] focus on optimizing 360-degree omnidirectional CP performance, aiming to extend an ego CAV's scope in every direction almost equally. However, this overlooks the uneven traffic density across different directions and the varying interest of an ego CAV in specific directions. For instance, as illustrated in Fig. 1, when an ego CAV is making a right turn at an intersection, it may encounter minimal traffic to its rear and left front, whereas the traffic is significantly more complex to its right front. In such scenarios, the ego CAV would benefit from a targeted perception enhancement towards its right front while maintaining basic (e.g., single-vehicle) perception for other directions. Existing methods aim to uniformly enhance perception across all directions, lacking the flexibility for an ego CAV to proactively adjust its view-level priority.

In addition, the communication overhead is critical factor that must be carefully considered when designing a CP system [2], [7]–[13]. With constraints such as a limited communication budget and a maximum allowable delay, engaging all collaborators and fully utilizing their captured views for enhancing perception across 360 degrees can significantly burden both communication and computational resources. This is particularly severe when the number of collaborators and the frame rate (measured in frames per second, FPS) are high. Indeed, reallocating communication resources from less critical directions to enhance perception in more important areas is not only strategically advantageous but

TABLE I

COMPARISON OF RELATED WORKS.

Method	Message	Fusion	Perception Gain
Who2com [14]	Full	Average	Omnidirectional
V2VNet [8]	Full	Average	Omnidirectional
PACP [1]	Full	Priority-based	Omnidirectional
When2com [5]	Full	Agent attention	Omnidirectional
V2X-ViT [15]	Full	Self-attention	Omnidirectional
Where2com [10]	Sparse	Location attention	Omnidirectional
Direct-CP (Ours)	Sparse	Proactive attention	**Directed**

also enhances CP efficiency in terms of both communication and computation.

Motivated by the above observation, we propose Direct-CP, which enables an ego CAV to proactively specify its interested directions and intelligently optimize perception performance toward these directions under the constraints of a limited communication budget. To achieve this, we plan to deploy several roadside units (RSUs) to monitor the traffic distribution around the ego CAV. These RSUs provide critical data that assists the ego vehicle in determining its interested directions. Additionally, we have developed a direction-aware attention module that inputs the ego CAV's preferred directions, communication budget, and the positional information of other CAVs, thereby generating sparse query maps that can intelligently select the most relevant information from nearby CAVs for aggregation to enhance CP performance toward selected directions. Moreover, we define a direction-weighted detection loss (DWLoss) to measure the directional perception discrepancy between prediction and ground truth. To the best of our knowledge, this is the first work designed to optimize CP based on local directional priorities. Our contributions can be summarized as follows.

- We propose a flexible CP framework named Direct-CP, which enhances perception performance towards specific directions under a limited communication budget, tailored to the proactive interests of an ego CAV.
- We design a direction-aware selective attention module to incorporate an RSU-aided direction masking mechanism, and adaptively select relevant feature data from multi-vehicle for boosting local-directional perception. Additionally, we design a direction-weighted detection loss (DWLoss) to measure the directed perception discrepancy between the outputs and the ground truth.
- We conduct extensive experiments on collaborative 3D detection tasks and the results demonstrate that our method realizes the proactive directed CP enhancement, achieving 2.5% higher overall perception accuracy and 19.8% higher local perception accuracy in the interested directions than the state-of-the-art method.

II. RELATED WORKS

A. Collaborative perception

Collaborative perception extends vehicles' sensing capabilities beyond individual sensor limits through intermediate-stage fusion strategies [16]–[20]. While this enables fea-

ture exchange among CAVs, increasing feature dimensions and collaborator numbers demand efficient bandwidth management. Who2com [14] employs a multi-stage handshake mechanism to compress information via matching scores, while V2VNet [8] uses graph neural networks to aggregate information from nearby CAVs. These methods, however, neglect the varying importance of individual CAVs. PACP [1] addresses this limitation with a BEV-match mechanism for CAV prioritization, but it only considers agent-level priorities while ignoring view-specific importance. Furthermore, PACP's focus on omnidirectional perception lacks the flexibility for directional perception adjustment, which is the focus of this paper.

B. Attention-based LiDAR perception

Recent advancements in LiDAR-based CP have integrated attention mechanisms to boost performance and reduce communication overhead. When2com [5] employs scaled general attention to assess correlations among different agents, reducing transmission redundancy. V2X-ViT [15] introduces the heterogeneous multi-agent attention for fusing messages across diverse agents. However, these methods require the initial transmission of full feature maps, which consumes substantial bandwidth. More recently, Where2comm [10] advances the field by utilizing sparse feature maps with location-specific and confidence-aware attention, optimizing data exchange and processing efficiency by focusing on the most relevant features. Despite its progress, Where2comm lacks the flexibility for an ego vehicle to adjust its perceptual focus based on immediate environmental demands and may not be optimal under limited communication conditions. As outlined in Table I, our proposed Direct-CP contrasts by providing a flexible and directed perception enhancement tailored to an ego vehicle's proactive needs under limited communication constraints. This targeted approach improves data relevance and efficiency, aligning closely with real-time needs in dynamic vehicular settings.

III. METHODOLOGY

Fig. 2 illustrates our method's architecture. RSUs deployed along the roadway monitor traffic from elevated positions, providing broader views than individual vehicles. The ego CAV periodically exchanges its status with nearby RSUs to receive direction attention scores (DAS). Based on DAS and its interests, the ego vehicle masks non-essential directions during collaborative perception. Then, guided by prioritized directions, communication budget, and neighboring CAVs' poses, it selects optimal feature map queries to maximize directed perception performance. The following subsections detail these components.

A. RSU-aided direction masking

In this paper, we leverage RSUs to help ego CAVs identify important directions. The 360-degree space around an ego CAV is divided into N_{dir} local directions. Based on ego CAV's location and speed, the corresponding RSU projects it into its captured 2D view and calculates Direction Attention
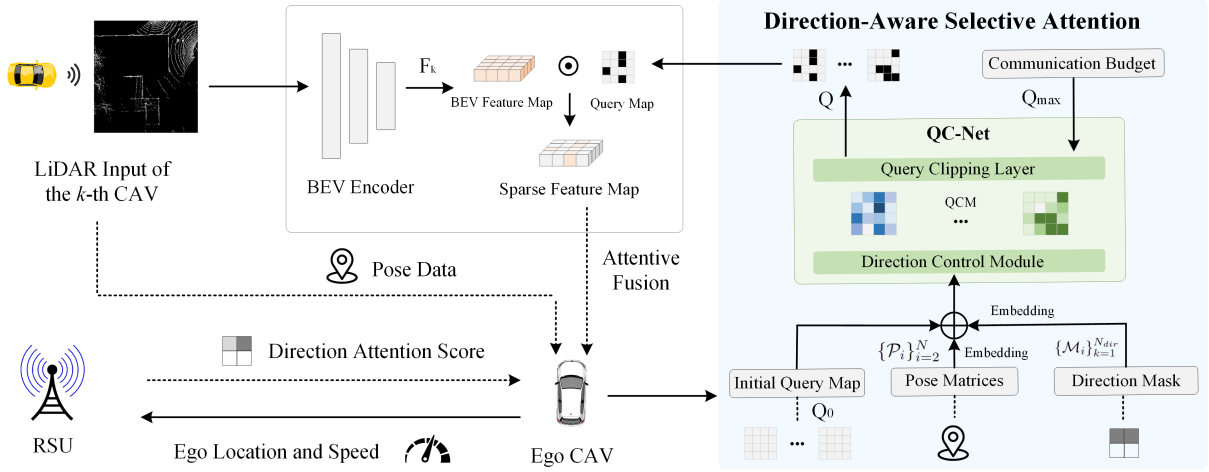
Fig. 2. **Method overview.** Ego CAV combines RSU's DAS with its interests to create direction mask. The mask, along with initial query map, neighboring CAVs' poses, and communication budget, are input to QC-Net. QC-Net contains: (i) **Direction Control Module** generating direction-prioritized query confidence maps (QCMs), and (ii) **Query Clipping Layer** selecting top $Q_{max} \times H \times W$ queries based on QCMs under budget constraints.

Scores (DAS) for each direction. For DAS calculation, we primarily use vehicle density as an indicator, as areas with higher vehicle density typically require more attention. The DAS from RSU is represented as $\{\mathcal{S}_r^i\}_{k=1}^{N_{dir}} = \{N_{vec}^i\}_{k=1}^{N_{dir}}$, where N_{vec}^i denotes the number of detected vehicles in the i-th direction. When RSU is unavailable, the system can alternatively use historical CP results to estimate traffic density, ensuring system robustness. This approach can be extended to incorporate additional factors such as vehicle speeds, accident history, and road conditions. The ego CAV then combines RSU's DAS $\{\mathcal{S}_r^i\}_{i=1}^{N_{dir}}$ with its own interest weights $\{\mathcal{I}_e^i\}_{i=1}^{N_{dir}}$ to calculate the final direction mask. These interest weights can be flexibly adjusted according to the ego vehicle's proactive needs. In cases where the weights are uniformly assigned, the direction importance relies entirely on RSU's DAS. The final direction mask $\{\mathcal{M}_i\}_{i=1}^{N_{dir}}$ is calculated as follows:

$$
\mathcal{M}_i = \max\left\{ H\left(\frac{\mathcal{S}_r^i \mathcal{I}_e^i}{\sum_{j=1}^{N_{dir}} \mathcal{S}_r^j \mathcal{I}_e^j} - \sigma_1\right), H(\mathcal{S}_r^i \mathcal{I}_e^i - \sigma_2) \right\},
$$
(1)

where Heaviside step function $H(\cdot)$ equals 1 for positive inputs and 0 otherwise. The threshold σ_1 determines the relative importance of each direction, while σ_2 serves as an absolute threshold to identify complex traffic scenarios even in relatively less important directions.

Our RSU-aided direction masking mechanism offers several key advantages. First, the communication between ego vehicle and RSU only involves basic information (location, speed, and DAS), ensuring minimal bandwidth usage and real-time performance. Second, the interest weight matrix provides ego vehicles with full autonomy in direction prioritization, allowing them to override RSU suggestions when necessary. Third, the dual-threshold design (σ_1 and σ_2) enables both relative and absolute traffic complexity assessment, enhancing the system's adaptability to various scenarios.

B. Direction-aware selective attention

Consider N CAVs in total in the scenario. Assume that the direction priority, the observation sets and perception supervision of the i-th CAV are represented as $\mathcal{M}_i$, $\mathcal{X}_i$ and $\mathcal{Y}_i$, respectively. The object of our considered directed collaborative perception system is to achieve the maximized perception performance toward interested directions of all agents as a function of communication budget B and the number of CAVs N, written as:

$$
\xi_\Phi(B, N) = \arg\max_{\theta, \mathcal{T}} \sum_{i=1}^{N} g\left(\Phi_\theta\left(\mathcal{X}_i, \{\mathcal{T}_{i,k}\}_{k=1}^N\right), \mathcal{M}_i, \mathcal{Y}_i\right),
$$
$$
\text{s.t.} \sum_{k=1}^{N} |\{\mathcal{T}_{i,k}\}_{k=1}^N| \le B,
$$
(2)

where $g(\cdot, \cdot)$ is the perception performance metric, Φ_θ is the perception model with trainable parameter θ, $\{\mathcal{T}_{i,k}\}_{k=1}^N$ are the messages transmitted from the k-th agent (each with M features) to the i-th agent. Note that the case when $N = 1$ indicates single-vehicle perception.

Upon receiving a 3D point cloud, the i-th CAV first converts the data into a BEV map. The BEV encoder Φ_{bev} processes this map to extract features, generating the feature map $\Phi_{bev}(\mathcal{X}_i) = \mathcal{F}_i \in \mathbb{R}^{H \times W \times D}$, where H, W, and D represent height, width, and channel dimensions, respectively. All agents project their perceptual data into a unified global coordinate system, facilitating seamless cross-agent collaboration without the need for complex coordinate transformations. The resulting feature map is fused with each other following direction-aware selective attention (DSA). The core component of DSA is the query-control net (QC-Net) taking initial query map $\mathcal{Q}_0 \in \mathbb{R}^{H \times W \times (N-1)}$, the embedding of nearby cooperative CAV's pose matrices $\text{PE}(\{\mathcal{P}_i\}_{i=2}^N) \in \mathbb{R}^{H \times W \times (N-1)}$, the embedding of ego CAV's direction mask $\text{DE}(\{\mathcal{M}_k\}_{k=1}^{N_{dir}}) \in \mathbb{R}^{H \times W \times (N-1)}$, and the communication budget as input, and generates proactive bi-

nary query maps $\{\mathcal{Q}_k\}_{k=2}^N \in \mathbb{R}^{H \times W \times (N-1)}$ (value 1 means activating transmitting data in the corresponding location of BEV feature map). The **communication budget** $Q_{max} \in [0,1]$ is defined as the ratio of the maximum number of activated queries to the size of the query map, which satisfies:

$$Q_{max} \geq \sum_{k=2}^{N} \sum_{i=1}^{H} \sum_{j=1}^{W} \frac{\mathcal{Q}_k^{i,j}}{H \times W \times (N-1)}, \qquad (3)$$

where $Q_{max} = 1$ means allowing CAVs to transmit full feature map to the ego vehicle. The QC-Net consists of a three-layer MLP. The direction control module first generates query confidence map (QCM) $\{\mathcal{C}_k\}_{k=2}^N \in \mathbb{R}^{H \times W \times (N-1)}$ for each CAV, while $\mathcal{C}_k^{i,j} \in [0,1]$ represents the priority of the j-th element of the i-th QCM for enhancing CP in the ego vehicle's interested directions. Assume the direction control module is denoted with $\Phi_{dcl}(\cdot)$, QCM is calculated by:

$$\{\mathcal{C}_k\}_{k=2}^N = \Phi_{dcl}\left(\mathcal{Q}_0, \mathrm{PE}(\{\mathcal{P}_i\}_{i=2}^N), \mathrm{DE}(\{\mathcal{M}_k\}_{k=1}^{N_{dir}})\right). \qquad (4)$$

Given communication constraints, we introduce a query clipping layer to control the transmitted data during the collaboration. In this layer, we rank $\mathcal{C}_k^{i,j}$ for each QCM, retaining only the top $Q_{max} \times H \times W$ values and setting others to zero, ensuring adherence to the predefined communication budget. The QC-Net finally produces sparse query maps $\{\mathcal{Q}_k\}_{k=2}^N$ as follows:

$$\mathcal{Q}_k^{i,j} = \begin{cases} 1, & \text{if } \mathcal{C}_k^{i,j} \in \mathrm{TOP}_{Q_{max} \times H \times W}\left(\{\mathcal{C}_k\}_{k=2}^N\right), \\ 0, & \text{otherwise,} \end{cases} \qquad (5)$$

where $\mathrm{TOP}_k(\cdot)$ reprsents the top k elements of a set.

Collaborative CAVs receive these query maps and compute direction-aware sparse feature maps as $\mathcal{H}_i = \mathcal{Q}_i \odot \mathcal{F}_i \in \mathbb{R}^{H \times W \times D}$, where $\odot$ denotes the Hadamard product of two matrices. Subsequently, each ego vehicle fuses features from multiple agents at each spatial location:

$$W_{i,j}^{DSA} = \mathrm{MAttn}\left(\mathcal{F}_i, \mathcal{H}_{i,j}, \mathcal{H}_{i,j}\right) \odot \mathcal{C}_j, \qquad (6)$$

where $W_{i,j}^{DSA} \in \mathbb{R}^{H \times W}$ is DSA weights assigned to the j-th agent by the i-th agent, $\mathrm{MAttn}(\cdot)$ represents the multi-head attention at each spatial location. The fused feature map for the ego vehicle $\mathcal{F}_i^{out} \in \mathbb{R}^{H \times W \times D}$ is expressed as:

$$\mathcal{F}_i^{out} = \mathrm{FFN}\left(\sum_{j=1}^{N} W_{i,j}^{DSA} \odot \mathcal{H}_{i,j}\right), \qquad (7)$$

where $\mathrm{FFN}(\cdot)$ is the feed-forward network.

C. Direction-weighted detection loss

Given the final fused feature map $\mathcal{F}_i^{out}$, the detection decoder $\Phi_{dec}(\cdot)$ generates class and regression outputs following [10]. Each output location $\Phi_{dec}(\mathcal{F}_i^{out}) \in \mathbb{R}^{H \times W \times 7}$ corresponds to a rotated box described by a 7-tuple $(c, x, y, h, w, \cos\alpha, \sin\alpha)$, representing class confidence, position, size, and angle. To evaluate the discrepancy between the collaborative 3D detection results and the ground truth, the commonly used detection loss $\mathcal{L}_{det}$ [21]
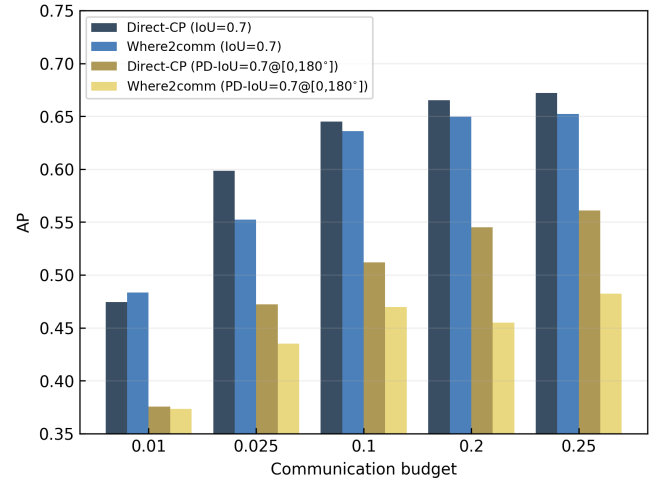

Fig. 3. **AP of different CP methods** under various communication budgets.

combines focal loss, object offset loss, and object size loss. However, this loss does not fully capture the importance of specific directions in our directed CP scenario. Therefore, we introduce a novel loss function, direction-weighted detection loss (DWLoss), to quantify the divergence in designated directions. DWLoss is calculated by dividing the 3D detection results into N_{dir} subsets and computing the detection loss $\{\mathcal{L}_{det}^i\}_{i=1}^{N_{dir}}$ for each subset with varying sum weights, represented as follows:

$$\mathcal{L}_{DW} = \frac{\sum_{i=1}^{N_{dir}} \mathcal{L}_{det}^i * (\mathcal{M}_i + \sigma)}{\sum_{i=1}^{N_{dir}} \mathcal{M}_i + \sigma N_{dir}}, \qquad (8)$$

where σ is a constant weight-control factor. Eq. 8 ensures setting lower weights to non-critical directions by weight factor σ, aiming to jointly optimize the CP performance in interested directions and the remaining directions. The choice of σ is crucial: setting it too high may obscure the importance of interested directions, while setting it too low (an extreme case is 0), can neglect the accuracy in non-critical directions during training, potentially degrading perception more than single-vehicle perception. Ablation studies in Section IV will offer helpful guidance for determining an effective σ.

IV. EXPERIMENTS

A. Experimental setup

Dataset and baselines. Our experimental evaluations are conducted on the V2X-Sim 2.0 Dataset [22], an extensive simulated dataset generated using the CARLA simulator [23]. This dataset comprises 10,000 frames of 3D LiDAR point clouds along with 501,000 annotated 3D bounding boxes. We configure the perception range to be $64m \times 64m$, and the 3D points are discretized into a BEV map of dimensions $(252, 100, 64)$. We establish baseline comparisons, including When2com [5], V2VNet [8], and Where2comm [10]. To make the perception gain clearer, we set the single-vehicle perception method as the lower-bound baseline.

Implementation details. We implement our Direct-CP using PyTorch. The direction control module features a fully

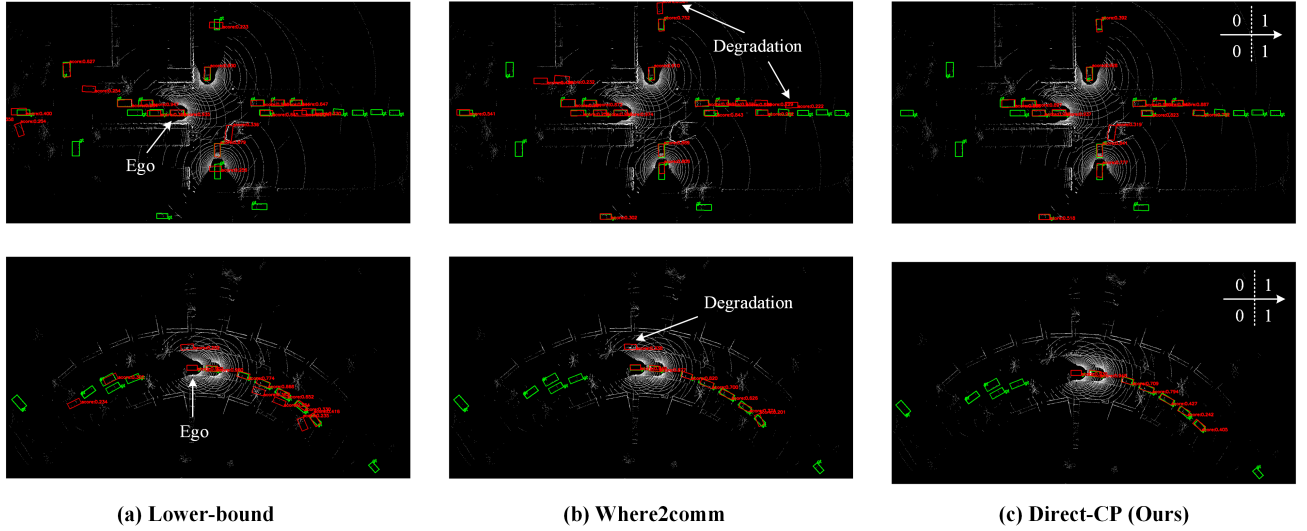**(a) Lower-bound** **(b) Where2comm** **(c) Direct-CP (Ours)**

Fig. 4. **Visualization comparison** on V2X-Sim 2.0 dataset. Green and red boxes denote ground truth and predictions, respectively. While Where2comm improves global perception over lower-bound, it shows limitations in certain directions. Direct-CP enhances perception in ego's interested directions (marked as 1, with right arrow showing ego's movement).

connected layer with dimensions of 100×252 for both input and output, complemented by a sigmoid layer to match the BEV feature dimensions, incorporating pose matrices and direction masks at a spatial resolution of $(100, 252)$. Our detection module utilizes the LiDAR-based 3D object detection framework PointPillar [24]. We set the training batch size at 6 and the maximum epochs at 60. The 360-degree space is divided into 4 directions: [0, 90°], [90°, 180°], [180°, 270°], and [270°, 360°], corresponding to left front, right front, right back, and left back, with interest weights of [0.9, 0.9, 0.1, 0.1], respectively. The default DWLoss weight factor σ is 1.0 and the default communication budget (defined in Eq. 3) is 0.2. The setup for our experiments includes 2 Intel(R) Xeon(R) Silver 4410Y CPUs (2.0GHz), 4 NVIDIA RTX A5000 GPUs, and 512GB DDR4 RAM.

Evaluation metrics. For 3D detection tasks, the intersection over union (IoU) is a common evaluation metric, calculated as the area of intersection divided by the area of union. However, IoU assesses omnidirectional perception performance. To specifically evaluate our proposed directed perception performance, we additionally introduce a metric named partial-direction intersection over union (PD-IoU). This involves dividing the BEV map into N_{dir} subsets based on predefined directions, with PD-IoU separately measuring IoU within these individual subsets.

B. Quantitative results

Evaluation of Direct-CP. We evaluate Direct-CP against baselines in the overall CP performance (AP@IoU=0.5/0.7) and in specific directions (AP@PD-IoU=0.5/0.7, interested directions are denoted with *). As shown in Table II, Direct-CP uses direction-aware selective attention to reallocate communication resources, slightly outperforming the state-of-the-art Where2comm in terms of overall AP@IoU. For PD-IoU, Where2comm optimizes CP omnidirectionally, showing

similar AP@PD-IoU across all directions, while Direct-CP focuses on preferred directions, achieving 18.2% higher AP@PD-IoU=0.5 and 19.8% higher AP@PD-IoU=0.7 than Where2comm in these directions. These results demonstrate that Direct-CP enables an ego vehicle to flexibly adjust view focus and improve CP performance in the desired directions.

Communication efficiency. Moreover, we investigate how varying communication budgets affects CP performance as shown in Fig. 3 with budgets ranging from 0.01 to 0.25. Notably, below a budget of 0.1, both Direct-CP and Where2comm experience a significant drop in AP@IoU=0.7 and AP@PD-IoU=0.7 for interested directions [0, 180°]. Despite this, Direct-CP slightly outperforms Where2comm overall and significantly improves perception in interested directions. At a further reduced budget of 0.01, both methods perform equally, suffering major perception degradation likely due to ultra-sparse feature maps impeding model convergence. Overall, these results highlight Direct-CP's efficiency under constrained communication resources.

Abalation studies. To investigate the influence of the weight factor σ on the performance of Direct-CP, we conduct an ablation study, varying σ from 0 to 2.0. When σ is below 1.0, we observe a reduction in collaborative detection accuracy, particularly in less critical directions. Notably, AP@PD-IoU=0.7 for the sector [270°, 360°] declines to 0.03, markedly deteriorating below the lower-bound threshold. Conversely, when σ exceeds 1.5, there is a discernible decrease in detection accuracy for both the areas of interest and the overall system. Based on these observations, a good range for σ is between 1.0 and 1.5, which balances directed perception performance with satisfactory overall accuracy.

C. Qualitative results

Visualization of collaborative 3D detection results. As shown in Fig. 4, we display Direct-CP's collaborative

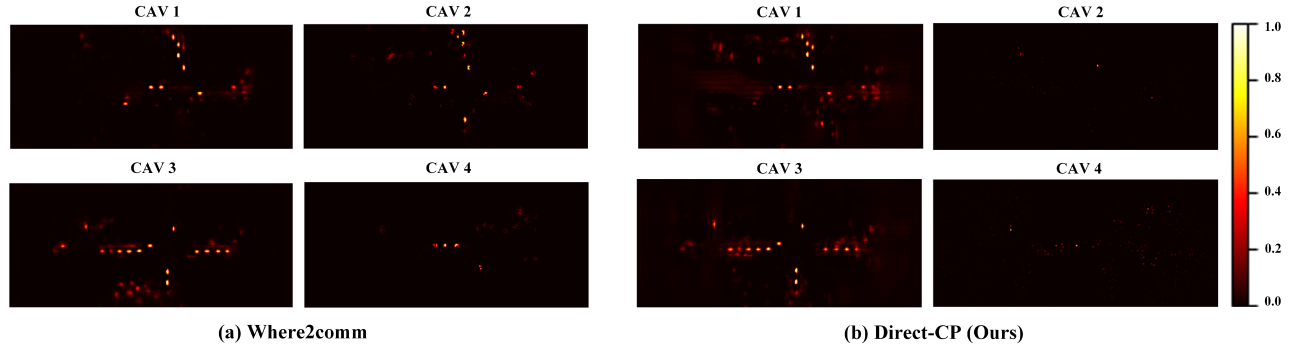**(a) Where2comm**   **(b) Direct-CP (Ours)**

Fig. 5. **Attention weight visualization** on neighboring CAVs. Where2comm distributes attention equally for omnidirectional perception, while Direct-CP focuses on features relevant to ego's interested directions.

TABLE II

QUANTITATIVE RESULTS OF COLLABORATIVE 3D DETECTION (COMMUNICATION BUDGET = 0.2). * INDICATES INTERESTED DIRECTIONS.

Method	AP@PD-IoU=0.5				AP@IoU=0.5	AP@PD-IoU=0.7				AP@IoU=0.7
	[0°,90°]*	[90°,180°]*	[180°,270°]	[270°,360°]		[0°,90°]*	[90°,180°]*	[180°,270°]	[270°,360°]	
Lower-bound	40.97	53.89	28.83	37.57	55.01	31.14	38.97	20.13	28.24	41.91
When2comm [5]	34.97	33.56	19.36	49.96	53.56	24.81	24.59	8.75	40.42	38.70
V2VNet [8]	57.49	53.62	28.01	60.36	67.35	42.61	41.05	19.54	36.59	48.22
Where2comm [10]	51.29	59.38	48.83	56.27	79.59	45.86	44.52	37.89	48.83	64.96
Direct-CP (Ours)	**65.84**$^{+28.4\%}$	**65.48**$^{+10.3\%}$	37.21	60.55	**81.17**$^{+2.0\%}$	**55.76**$^{+21.6\%}$	**53.20**$^{+19.5\%}$	28.62	49.98	**66.57**$^{+2.5\%}$

TABLE III

ABLATION STUDIES ON THE EFFECT OF DWLOSS WEIGHT FACTOR σ (COMMUNICATION BUDGET = 0.2). * INDICATES INTERESTED DIRECTIONS.

Direct-CP	AP@PD-IoU=0.5				AP@IoU=0.5	AP@PD-IoU=0.7				AP@IoU=0.7
	[0°,90°]*	[90°,180°]*	[180°,270°]	[270°,360°]		[0°,90°]*	[90°,180°]*	[180°,270°]	[270°,360°]	
$\sigma = 0$	38.28	51.37	30.71	27.12	61.63	14.84	29.16	14.75	3.38	31.41
$\sigma = 0.5$	59.83	59.12	36.66	58.30	76.19	41.03	44.85	25.72	46.24	58.18
$\sigma = 1.0$	**65.84**	**65.48**	37.21	**60.55**	**81.17**	**55.76**	**53.20**	28.62	**49.98**	**66.57**
$\sigma = 1.5$	52.86	62.98	**41.49**	55.78	73.94	44.81	51.90	**34.93**	47.84	62.12
$\sigma = 2.0$	49.24	62.46	32.23	55.14	73.21	36.97	48.21	25.51	42.90	57.18

detection results alongside baselines on the V2X-Sim 2.0 dataset. While Where2comm substantially improves global perception over the lower-bound, it underperforms in certain local directions, occasionally not exceeding single-vehicle outcomes, likely due to limited communication budgets and scattered focus. Conversely, our Direct-CP effectively redirects attention from less critical to key areas, significantly boosting local directional perception.

Visualization of ego CAV's attention weights. As depicted in Fig. 5, we further compare the attention weights of ego CAV assigned to neighboring CAVs' feature maps $W_{i,j}^{DSA}$ (defined in Eq. 6) in two methods. With limited communication budgets, both methods query sparse features. For Where2comm, the attention weights are more uniformly assigned to other CAVs to enhance 360-degree CP performance. In contrast, our proposed Direct-CP attends to features that are more crucial to the ego vehicle's interested directions, informed by other CAVs' pose information and the ego's directional mask, shifting great attention from CAV 2 and 4 to CAV 1 and 3 to improve directed CP performance.

V. CONCLUSION

In this paper, we have introduced Direct-CP, a novel CP system for ego vehicles to enhance perception in patronized directions. We have developed RSU-aided direction masking by integrating RSU's traffic detection with ego vehicle's interests to identify key directions. We have also designed a proactive direction-aware attention mechanism to collect sparse feature maps from multiple vehicles under limited communication budgets, improving local directional perception. Additionally, we have created a direction-weighted detection loss to align perception outputs with ground truth. Extensive experiments demonstrate that Direct-CP achieves directed performance gains under constrained communication resources and outperforms baselines in efficiency. Looking forward, our direction-aware framework opens new possibilities for adaptive perception, and future work could explore incorporating sophisticated traffic indicators and extending to extreme weather conditions and complex urban environments.

REFERENCES

[1] Z. Fang, S. Hu, H. An, Y. Zhang, J. Wang, H. Cao, X. Chen, and Y. Fang, " PACP: Priority-Aware Collaborative Perception for Connected and Autonomous Vehicles ," *IEEE Transactions on Mobile Computing*, vol. 23, no. 12, pp. 15 003–15 018, Dec. 2024.

[2] S. Hu, Z. Fang, X. Chen, Y. Fang, and S. Kwong, "Towards Full-scene Domain Generalization in Multi-agent Collaborative Bird's Eye View Segmentation for Connected and Autonomous Driving," 2024. [Online]. Available: https://arxiv.org/abs/2311.16754

[3] Y. Zhang, H. An, Z. Fang, G. Xu, Y. Zhou, X. Chen, and Y. Fang, "SmartCooper: Vehicular Collaborative Perception with Adaptive Fusion and Judger Mechanism," in *IEEE International Conference on Robotics and Automation (ICRA)*, Yokohama, Japan, May 2024.

[4] Z. Liu, H. Tang, A. Amini, X. Yang, H. Mao, D. L. Rus, and S. Han, "BEVFusion: Multi-Task Multi-Sensor Fusion with Unified Bird's-Eye View Representation," in *IEEE International Conference on Robotics and Automation (ICRA)*, 2023, pp. 2774–2781.

[5] Y.-C. Liu, J. Tian, N. Glaser, and Z. Kira, "When2com: Multi-Agent Perception via Communication Graph Grouping," in *Proceedings of the IEEE/CVF Conference on Computer Vision and Pattern Recognition (CVPR)*, June 2020.

[6] Y. Li, S. Ren, P. Wu, S. Chen, C. Feng, and W. Zhang, "Learning Distilled Collaboration Graph for Multi-Agent Perception," in *Advances in Neural Information Processing Systems (NeurIPS)*, A. Beygelzimer, Y. Dauphin, P. Liang, and J. W. Vaughan, Eds., 2021.

[7] Y.-C. Liu, J. Tian, C.-Y. Ma, N. Glaser, C.-W. Kuo, and Z. Kira, "Who2com: Collaborative Perception via Learnable Handshake Communication," in *IEEE International Conference on Robotics and Automation (ICRA)*, 2020, pp. 6876–6883.

[8] T.-H. Wang, S. Manivasagam, M. Liang, B. Yang, W. Zeng, and R. Urtasun, "V2VNet: Vehicle-to-Vehicle Communication for Joint Perception and Prediction," in *European Conference on Computer Vision (ECCV)*. Berlin, Heidelberg: Springer-Verlag, 2020, pp. 605–621.

[9] S. Hu, Z. Fang, Y. Deng, X. Chen, and Y. Fang, "Collaborative Perception for Connected and Autonomous Driving: Challenges, Possible Solutions and Opportunities," Jan. 2024, arXiv:2401.01544 [cs, eess].

[10] Y. Hu, S. Fang, Z. Lei, Y. Zhong, and S. Chen, "Where2comm: Communication-Efficient Collaborative Perception via Spatial Confidence Maps," in *Advances in Neural Information Processing Systems (NeurIPS)*, A. H. Oh, A. Agarwal, D. Belgrave, and K. Cho, Eds., 2022.

[11] S. Hu, Z. Fang, Z. Fang, Y. Deng, X. Chen, and Y. Fang, "AgentsCo-Driver: Large Language Model Empowered Collaborative Driving with Lifelong Learning," Apr. 2024, arXiv:2404.06345 [cs].

[12] S. Hu, Z. Fang, Z. Fang, Y. Deng, X. Chen, Y. Fang, and S. Kwong, "AgentsCoMerge: Large Language Model Empowered Collaborative Decision Making for Ramp Merging," 2024. [Online]. Available: https://arxiv.org/abs/2408.03624

[13] Z. Fang, J. Wang, Y. Ren, Z. Han, H. V. Poor, and L. Hanzo, "Age of information in energy harvesting aided massive multiple access networks," *IEEE Journal on Selected Areas in Communications*, vol. 40, no. 5, pp. 1441–1456, May 2022.

[14] Y.-C. Liu, J. Tian, C.-Y. Ma, N. Glaser, C.-W. Kuo, and Z. Kira, "Who2com: Collaborative Perception via Learnable Handshake Communication," 2020. [Online]. Available: https://arxiv.org/abs/2003.09575

[15] R. Xu, H. Xiang, Z. Tu, X. Xia, M.-H. Yang, and J. Ma, "V2X-ViT: Vehicle-to-Everything Cooperative Perception with Vision Transformer," in *European Conference on Computer Vision (ECCV)*. Berlin, Heidelberg: Springer-Verlag, 2022, p. 107–124. [Online]. Available: https://doi.org/10.1007/978-3-031-19842-7_7

[16] Y. Zhou, J. Xiao, Y. Zhou, and G. Loianno, "Multi-Robot Collaborative Perception With Graph Neural Networks," *IEEE Robotics and Automation Letters*, vol. 7, no. 2, pp. 2289–2296, 2022.

[17] Y. Lu, Q. Li, B. Liu, M. Dianati, C. Feng, S. Chen, and Y. Wang, "Robust Collaborative 3D Object Detection in Presence of Pose Errors," in *IEEE International Conference on Robotics and Automation (ICRA)*, 2023, pp. 4812–4818.

[18] S. Su, Y. Li, S. He, S. Han, C. Feng, C. Ding, and F. Miao, "Uncertainty Quantification of Collaborative Detection for Self-Driving," in *IEEE International Conference on Robotics and Automation (ICRA)*, 2023, pp. 5588–5594.

[19] R. Xu, W. Chen, H. Xiang, X. Xia, L. Liu, and J. Ma, "Model-Agnostic Multi-Agent Perception Framework," in *IEEE International Conference on Robotics and Automation (ICRA)*, 2023, pp. 1471–1478.

[20] R. Xu, J. Li, X. Dong, H. Yu, and J. Ma, "Bridging the Domain Gap for Multi-Agent Perception," in *IEEE International Conference on Robotics and Automation (ICRA)*, 2023, pp. 6035–6042.

[21] X. Zhou, D. Wang, and P. Krähenbühl, "Objects as Points," 2019. [Online]. Available: https://arxiv.org/abs/1904.07850

[22] Y. Li, D. Ma, Z. An, Z. Wang, Y. Zhong, S. Chen, and C. Feng, "V2X-Sim: Multi-Agent Collaborative Perception Dataset and Benchmark for Autonomous Driving," 2022. [Online]. Available: https://arxiv.org/abs/2202.08449

[23] A. Dosovitskiy, G. Ros, F. Codevilla, A. Lopez, and V. Koltun, "CARLA: An open urban driving simulator," in *Proceedings of the 1st Annual Conference on Robot Learning*, ser. Proceedings of Machine Learning Research, S. Levine, V. Vanhoucke, and K. Goldberg, Eds., vol. 78. PMLR, 13–15 Nov 2017, pp. 1–16.

[24] A. H. Lang, S. Vora, H. Caesar, L. Zhou, J. Yang, and O. Beijbom, "PointPillars: Fast Encoders for Object Detection From Point Clouds," in *Proceedings of the IEEE/CVF Conference on Computer Vision and Pattern Recognition (CVPR)*, June 2019.